International Journal of Mechanical, Industrial and Aerospace Sciences
ISSN: 2517-9950
Vol:7, No:5, 2013

Lateral and Longitudinal Vibration of a Rotating Flexible Beam Coupled with Torsional Vibration of a Flexible Shaft

Khaled Alnefaie

***Abstract*—**In this study, rotating flexible shaft-disk system having flexible beams is considered as a dynamic system. After neglecting nonlinear terms, torsional vibration of the shaft-disk system and lateral and longitudinal vibration of the flexible beam are still coupled through the motor speed. The system has three natural frequencies; the flexible shaft-disk system torsional natural frequency, the flexible beam lateral and longitudinal natural frequencies. Eigenvalue calculations show that while the shaft speed changes, torsional natural frequency of the shaft-disk system and the beam longitudinal natural frequency are not changing but the beam lateral natural frequency changes. Beam lateral natural frequency stays the same as the nonrotating beam lateral natural frequency ω_b until the motor speed ω_m is equal to ω_b. After then ω_b increases and remains equal to the motor speed ω_m until the motor speed is equal to the shaft-disk system natural frequency ω_T. Then the beam lateral natural frequency ω_b becomes equal to the natural frequency ω_T and stays same while the motor speed ω_m is increased. Modal amplitudes and phase angles of the vibrations are also plotted against the motor speed ω_m.

***Keywords*—**Rotor dynamics, beam-shaft coupling, beam vibration, flexible shaft.

I. Introduction

VIBRATION problem of rotating beams has been a subject of extensive research due to a number of very important applications such as helicopter blades, turbine blades, and appendages of spinning satellites. References [7], [8], [10] have studied a model consisting of servomotor, harmonic drive, flexible shaft and a rigid manipulator arm. Transfer function of the system relating desired input rotation to the manipulator arm rotation is developed. Flexible system natural frequency and damping ratio together with PID control parameters appear in the transfer function. The possibility of a precise trajectory tracking is discussed and frequency response characteristics of the system with respect to some parameters are studied. Reference [5] have also modeled rotating Euler-Bernoulli type beam and studied residual vibration spectrum of the beam. It is shown that at certain frequencies of the rise function, residual vibration can be eliminated. For the same model shear force at the root of the beam is used as a feedback for the control system and parametric analysis is done, the effect of shear force feedback control strategy on the beam tip vibration is studied. . References [12], [13] have studied coupling effect of a flexible link and a flexible joint in one-link rotating structure. Two nondimensional parameters are defined; the ratio of a bending stiffness of the link to the torsional stiffness of the rotor and the ratio of moment of inertia of the link to the rotor. Unconstrained and constrained modal expansions are compared. Reference [2] has developed general model to describe the rotating blade vibration under the effect of shaft torsional vibration. Reference [1] have studied mathematical model for a flexible arm undergoing large planar flexural deformation, continuously rotating under the effect of a hub torque and supported by a flexible base. Reference [3] have developed a new approach based on a linear quadratic estimator technique for estimating the vibration of any point on the span of a rotating flexible beam mounted on a compliant hub in the presence of process and measurement noise. Reference [11] have studied coupled nonlinear equations of motion of a coupled elastic shaft-elastic beam model in a very general fashion considering the influence of rotor, shaft, hub, beam and payload as well as geometric stiffness terms which arise from both centripetal and Coriolis accelerations. Their solution concentrates on the effect of two parameters representing the mass and stiffness ratios of the manipulator system on its driveline. References [4], [6], [9] analyzed a servomotor driven coupled elastic shaft–elastic beam system. The model consists of a servomotor, disk, and an elastic beam attached to the disk and separated by an elastic shaft. Equations of motion are derived with respect to the generalized coordinates of the elastic shaft, elastic beam and the servomotor rotation. Nonlinear terms coming from Coriolis, normal and tangential accelerations are retained in the equations. Change of eigenvalues of the system with respect to the control parameters and also beam tip vibrations are investigated.

In this study, rotating flexible shaft-disk system having flexible beams is considered as a dynamic system. Equations of the dynamic system are derived considering that the shaft is driven with a motor. After neglecting nonlinear terms, torsional vibration of the shaft-disk system and lateral and longitudinal vibration of the flexible beam are still coupled through the motor speed. The change of natural frequencies and modal amplitudes of the system are investigated with respect to the motor speed.

Khaled Alnefaie is with the Department of Mechanical Engineering, Faculty of Engineering, King Abdulaziz University, P.O. Box 80248, Jeddah 21589, Saudi Arabia. (e-mail: kalnefaie@kau.edu.sa).

II. Formulation

Fig. 1 shows the dynamic system consists of a disk having flexible beams circumferentially connected to it and the disk is connected a motor through flexible shaft. J_m is the motor inertia, J_d is the disk inertia, l_b is the beam length, l_s is the shaft length, θ_m , θ_s and θ_d are the motor, flexible shaft and disk rotation, respectively. Front view of the system shows the configuration of the disk and the flexible beam. OXY is the fixed frame of reference, Oxy is the rotating frame attached to the disk at disk center. r_d + x +$u(x,t)$ and $y(x,t)$ are the coordinates of the flexible beam unit mass m with respect to the rotating coordinates Oxy. $u(x,t)$ and $y(x,t)$ are the longitudinal and lateral displacements of unit mass m.

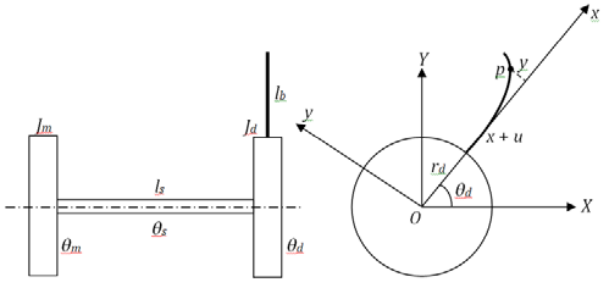

Fig. 1 Model of elastic shaft-disk-elastic beam system

The kinetic energy of the system can be written as

$$T = (1/2)J_m\dot{\theta}_m^2 + (1/2)J_d\dot{\theta}_d^2 + N\int_{r_d}^{r_d+l_b}(1/2)mv^2(x,t)dx + (1/2)\int_0^{l_s}\rho I_p\dot{\theta}_s^2(z,t)dz \quad (1)$$

In (1) N is the number of flexible beams attached to the disk, v is the velocity of the unit mass m, ρ is the density of beam material, I_p is the polar moment of inertia of the flexible shaft. The potential energy of the system can be written as

$$U = (1/2)N\int_{r_d}^{r_d+l_b}EIy''^2(x,t)dx + (1/2)\int_0^{l_s}GI_p\psi'^2(z,t)dz + (1/2)N\int_{r_d}^{r_d+l_b}EAu'^2(x,t)dx \quad (2)$$

In (2) EI is the rigidity of the elastic beam, GI_p is the rigidity of the elastic shaft, EA is the longitudinal rigidity of the beam, $\psi(z,t)$ is the elastic rotation of the shaft. The disk and the shaft rotation can be written as the sum of the motor rotation and the flexible shaft rotation as

$$\theta_s(z,t) = \theta_m(t) + \psi(z,t)$$
$$\theta_d(t) = \theta_m(t) + \psi(l_s,t) \quad (3)$$

It is assumed that the elastic motion of the beam and the shaft are sum of the orthogonal modes

$$\psi(z,t) = \sum_{i=1}^{n}\phi_{si}(z)q_{si}(t) \approx \phi_s(z)q_s(t)$$
$$y(x,t) = \sum_{i=1}^{n}\phi_{bi}(x)q_{bi}(t) \approx \phi_b(x)q_b(t) \quad (4)$$
$$u(x,t) = \sum_{i=1}^{n}\phi_{ui}(x)q_{ui}(t) \approx \phi_u(x)q_u(t)$$

Here $\phi_{si}(z)$, $\phi_{bi}(x)$ and $\phi_{ui}(x)$ are orthogonal modes, $q_{si}(t)$, $q_{bi}(t)$ and $q_{ui}(t)$ are generalized coordinates of the elastic shaft and elastic beam, respectively. In the following derivations, only first mode is considered.

Position vector of the beam unit mass m can be written as

$$\vec{r} = (r_d + x + u)\vec{i} + y\vec{j} \quad (5)$$

The velocity of the unit mass m can be found by taking time derivative of the vector $\vec{r}$ which is

$$v = \dot{\vec{r}} = (\dot{u} + y\dot{\theta}_d)\vec{i} + \left[(r_d + x + u)\dot{\theta}_d + \dot{y}\right]\vec{j} \quad (6)$$

If (3), (4) and (6) are used the kinetic and the potential energies of (1) and (2) will be

$$T = (1/2)J_m\dot{\theta}_m^2 + (1/2)J_d(\dot{\theta}_m + \bar{\phi}_s\dot{q}_s)^2 + (1/2)N\int_{r_d}^{r_d+l_b}m\left\{\begin{array}{l}\left[\phi_u\dot{q}_u + \phi_b q_b(\dot{\theta}_m + \bar{\phi}_s\dot{q}_s)\right]^2 + \\ \left[(r_d + x + \phi_u q_u)(\dot{\theta}_m + \bar{\phi}_s\dot{q}_s) + \phi_b\dot{q}_b\right]^2\end{array}\right\}dx + (1/2)\int_0^{l_s}\rho I_p(\dot{\theta}_m + \bar{\phi}_s\dot{q}_s)^2dz \quad (7)$$

$$U = (1/2)N\int_{r_d}^{r_d+l_b}EI\phi_b''^2q_b^2dx + (1/2)\int_0^{l_s}GI_p\phi_s'^2q_s^2dz + (1/2)N\int_{r_d}^{r_d+l_b}EA\phi_u'^2q_u^2dx \quad (8)$$

In (7) $\bar{\phi}_s = \phi(l_s)$. Lagrange equations are used to obtain dynamic equations of the system with respect to the generalized coordinates. Viscous damping is introduced through ζ_b , ζ_u and ζ_s which are lateral, longitudinal and torsional motion damping ratios, respectively. After ignoring nonlinear terms, the following equations are obtained

$$\ddot{\bar{q}}_b + 2\zeta_b\omega_b\dot{\bar{q}}_b + (\omega_b^2 + \omega_m^2)\bar{q}_b + (\lambda\alpha_1 + \alpha_2)\bar{\phi}_s\ddot{q}_s + 2\alpha_6\omega_m\dot{q}_u = 0 \quad (9)$$

$$\ddot{\bar{q}}_u + 2\zeta_u\omega_u\dot{\bar{q}}_u + (\omega_u^2 + \omega_m^2)\bar{q}_u + 2(\lambda\alpha_8 + \alpha_9)\bar{\phi}_s\omega_m\dot{q}_s + \alpha_7\omega_m\dot{q}_b = (\lambda\alpha_8 + \alpha_9)\omega_m^2 \quad (10)$$

$$\{(J_d/J_s)\alpha_5+(NJ_{b0}/J_s)\alpha_5+1\}\ddot{q}_s+2\zeta_s\omega_s\dot{q}_s+\omega_s^2\dot{q}_s+$$
$$(Nm_bl_b^2/J_s)(\lambda\alpha_3+\alpha_4)\bar{\phi}_s\ddot{q}_b+ \quad (11)$$
$$(2Nm_bl_b^2/J_s)(\lambda+(1/2))\alpha_5\omega_m\dot{q}_u=0$$

In these equations ω_m is the motor speed, ω_b and ω_u are the first natural frequencies of lateral and longitudinal vibrations of the beam and ω_s is the torsional vibration natural frequency of the elastic shaft. The following are definitions of other parameters

$$\bar{q}_b=q_b/l_b,\ \bar{q}_u=q_u/l_b,\ \lambda=r_d/l_b,$$
$$\alpha_1=\int_0^1\phi_b d\xi\Big/\int_0^1\phi_b^2 d\xi,\ \alpha_2=\int_0^1\phi_b\xi d\xi\Big/\int_0^1\phi_b^2 d\xi,$$
$$\alpha_3=\int_0^1\phi_b d\xi\Big/\int_0^1\phi_s^2 d\xi,\ \alpha_4=\int_0^1\phi_b\xi d\xi\Big/\int_0^1\phi_s^2 d\xi,$$
$$\alpha_5=\bar{\phi}_s^2\Big/\int_0^1\phi_s^2 d\xi,$$
$$\alpha_6=\int_0^1\phi_u\phi_b d\xi\Big/\int_0^1\phi_b^2 d\xi,\ \alpha_7=\int_0^1\phi_u\phi_b d\xi\Big/\int_0^1\phi_u^2 d\xi,$$
$$\alpha_8=\int_0^1\phi_u d\xi\Big/\int_0^1\phi_u^2 d\xi,\ \alpha_9=\int_0^1\phi_u\xi d\xi\Big/\int_0^1\phi_u^2 d\xi \quad (12)$$

$$d\xi=dx/l_b \text{ or } d\xi=dz/l_s,\ J_s=\int_0^{l_s}\rho I_p dz,$$
$$J_{b0}=\int_0^{l_b}m(r_d+x)^2dx,\ m_b=ml_b \quad (13)$$

Since the root of the flexible beam cannot be considered fixed because of the elastic rotation of the shaft, the characteristic equation of the lateral vibration of Euler-Bernoulli beam can be obtained by using the following boundary conditions

$$y(0,t)=0,\ EIy''(0,t)=(GI_p/l_s)y'(0,t),$$
$$y''(l_b,t)=0,\ y'''(l_b,t)=0 \quad (14)$$

The characteristic equation is

$$K(\cosh\beta_b l_b\cos\beta_b l_b+1)+$$
$$\beta_b l_b(\sinh\beta_b l_b\cos\beta_b l_b-\cosh\beta_b l_b\sin\beta_b l_b)=0 \quad (15)$$

Here K defined as rigidity factor, which is the ratio of the torsional stiffness of the shaft per unit length to the bending stiffness of the beam per unit length.

$$K=\frac{GI_p/l_s}{EI/l_b} \quad (16)$$

If the torsional stiffness of the shaft is infinite, the rigidity factor is infinite which corresponds to a fixed-free beam. If the torsional stiffness of the shaft is zero the rigidity factor is zero which corresponds to a hinged-free beam.

Depending on the value of the rigidity factor, the beam lateral natural frequency will be between the natural frequency of fixed-free beam and hinged-free beam.

For a given rigidity factor K, (15) can be solved and the lateral natural frequency of the beam can be calculated as

$$\omega_b=(\beta_b l_b)^2\sqrt{EI_b/ml_b^4} \quad (17)$$

For the longitudinal vibration of the beam the fixed-free boundary conditions are assumed as

$$u(0,t)=0,\ u'(l_b,t)=0 \quad (18)$$

Then the characteristic equation of the longitudinal vibration of the beam will be

$$(\omega/c)\cos(\omega l_b/c)=0,\ c=\sqrt{E/\rho} \quad (19)$$
$$\omega_u=(\pi/2)\sqrt{E/\rho l_b^2} \quad (20)$$

Concerning boundary conditions of the elastic shaft at the disk end, restoring moment is equal to the total inertial moment of the shaft, disk and beams.

$$GI_p\frac{\partial\psi(l_s)}{\partial z}=J_T\omega_s^2\psi(l_s) \quad (21)$$
$$J_T=J_s+J_d+NJ_{b0} \quad (22)$$

Characteristic equation of the torsional vibration of elastic shaft will be

$$\beta_s\tan\beta_s=J_s/J_T \quad (23)$$

then torsional natural frequency of the shaft is

$$\omega_s=\beta_s\sqrt{G/\rho l_s^2} \quad (24)$$

III. Simulations

Parameters selected for the simulations are listed in Table I.

TABLE I
Simulation Parameters

Symbol	Quantity	Value
r_d	disk radius	0.5 m
m_d	disk mass	120 kg
l_s	beam length	1.0 m
w_b x h_b	beam width x height	0.020 x 0.005 m
l_s	shaft length	0.1, 0.5, 1.0 m
d_s	shaft diameter	0.06 m
E	modulus of elasticity	207 GPa
G	modulus of shear	79 GPa

ρ	density of steel	7700 kg m^{-3}
ζ	damping factors	0.02

Three shaft lengths are used for the simulation; 0.1 m, 0.5 m, and 1.0 m. Beam lateral and longitudinal natural frequencies, shaft torsional natural frequency and shaft-disk system torsional natural frequency with respect to the three different shaft lengths are tabulated in Table II.

TABLE II
NATURAL FREQUENCIES OF THE SYSTEM FOR THREE DIFFERENT SHAFT LENGTHS

l_s (m)	K	ω_b (rad/s)	ω_u (rad/s)	ω_s (rad/s)	ω_T (rad/s)
0.1	23308	26.3	8144.4	50314	225.6
0.5	4662	26.3	8144.4	10063	100.9
1.0	2331	26.3	8144.4	5031	71.3

Equations of the system given in (9), (10) and (11) can be put in a matrix form

$$[M]\{\ddot{q}\}+[C]\{\dot{q}\}+[K]\{q\}=\{F\} \tag{25}$$

In open form, equations are

$$\begin{bmatrix} 1 & 0 & M_{13} \\ 0 & 1 & 0 \\ M_{31} & 0 & M_{33} \end{bmatrix}\begin{Bmatrix} \ddot{\bar{q}}_b \\ \ddot{\bar{q}}_u \\ \ddot{q}_s \end{Bmatrix}+\begin{bmatrix} 2\zeta_b\omega_b & C_{12} & 0 \\ C_{21} & 2\zeta_u\omega_u & C_{23} \\ M_{31} & C_{32} & 2\zeta_s\omega_s \end{bmatrix}\begin{Bmatrix} \dot{\bar{q}}_b \\ \dot{\bar{q}}_u \\ \dot{q}_s \end{Bmatrix}+ \begin{bmatrix} \omega_b^2+\omega_m^2 & C_{12} & 0 \\ C_{21} & \omega_u^2+\omega_m^2 & C_{23} \\ M_{31} & C_{32} & \omega_s^2 \end{bmatrix}\begin{Bmatrix} \bar{q}_b \\ \bar{q}_u \\ q_s \end{Bmatrix}=\begin{Bmatrix} 0 \\ f_2 \\ 0 \end{Bmatrix} \tag{26}$$

Terms M_{13}, M_{31}, M_{33}, C_{12}, C_{21}, C_{23}, C_{32} and f_2 can be found in (9), (10) and (11). There is a dynamic coupling through mass matrix elements M_{13}, M_{31}, but they are constant. There is no static coupling through stiffness matrix [K] but there are coupling terms in the damping matrix [C] through C_{12}, C_{21}, C_{23} and C_{32} and they are functions of motor speed ω_m. The eigenvalues of (25) can be found by constructing the system matrix, which is

$$[A]=\begin{bmatrix} 0 & I \\ -M^{-1}K & -M^{-1}C \end{bmatrix} \tag{27}$$

Solution of the system matrix will produce three pairs of complex eigenvalues, which are

$$\begin{aligned} s_{1,2} &= -\zeta_b\omega_b \pm \omega_b\sqrt{1-\zeta_b^2}\,j \\ s_{3,4} &= -\zeta_u\omega_u \pm \omega_u\sqrt{1-\zeta_u^2}\,j \\ s_{5,6} &= -\zeta_s\omega_T \pm \omega_T\sqrt{1-\zeta_s^2}\,j \end{aligned} \tag{28}$$

Since the roots are functions of the motor speed ω_m, for each given ω_m; ζ_b, ω_b, ζ_u, ω_u, ζ_s and ω_T can be calculated. Preliminary calculations show that the roots are sensitive to shaft length that is why the calculations are carried out for three different shaft lengths of 0.1m, 0.5m and 1.0m. Table II lists the rigidity factor K, the beam lateral natural frequency ω_b, the beam longitudinal natural frequency ω_u, the shaft torsional natural frequency ω_s and the torsional natural frequency of the shaft-disk system ω_T. Since the rigidity factor is very high for all shaft lengths, beam lateral natural frequency is not affected with the selected shaft lengths.

Fig. 2 shows how the lateral natural frequency ω_b changes with the motor speed. When the motor speed is zero, nonrotating beam lateral natural frequency ω_b is 26.3 rad/s for all shaft lengths. ω_b stays the same as the nonrotating beam lateral natural frequency until the motor speed ω_m is equal to ω_b. Then, ω_b starts increasing but remains equal to the motor speed ω_m until the motor speed is equal to the shaft-disk system natural frequency ω_T. After then the beam lateral natural frequency ω_b becomes equal to the shaft-disk system natural frequency ω_T and stays same while the motor speed ω_m is increased.

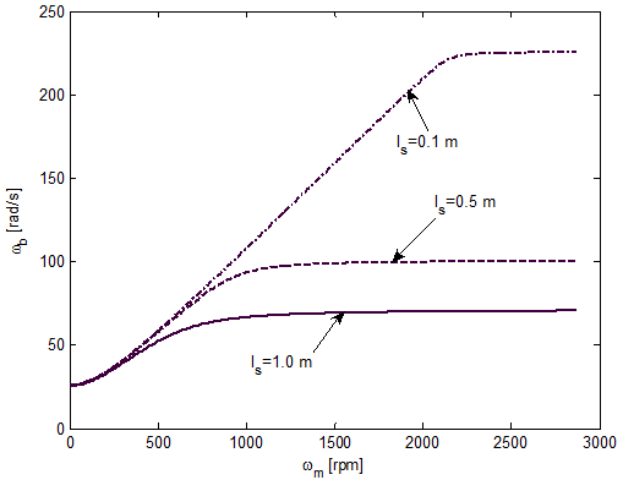

Fig. 2 The beam lateral natural frequency with respect to motor speed

Fig. 3 shows how beam lateral vibration damping ratio ζ_b is changing with the motor speed. Nonrotational damping ratio of 0.02 is assumed. While the motor speed is increased damping ratio decreases, when the motor speed reaches to shaft-disk system natural frequency ω_T increases back to its original value. For shorter shaft lengths, damping ratio is lowered more.

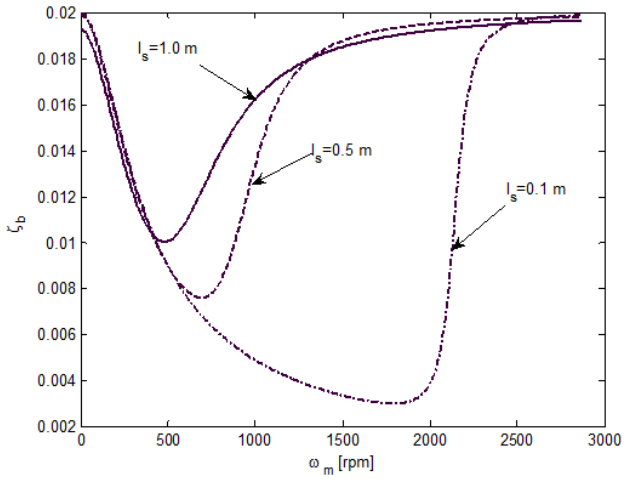

Fig. 3 The beam lateral vibration damping ratio with respect to motor speed

Fig. 4 shows the settling time of the beam lateral vibration. The settling time is defined as

$$t_s = \frac{4}{\zeta_b \omega_b} \tag{29}$$

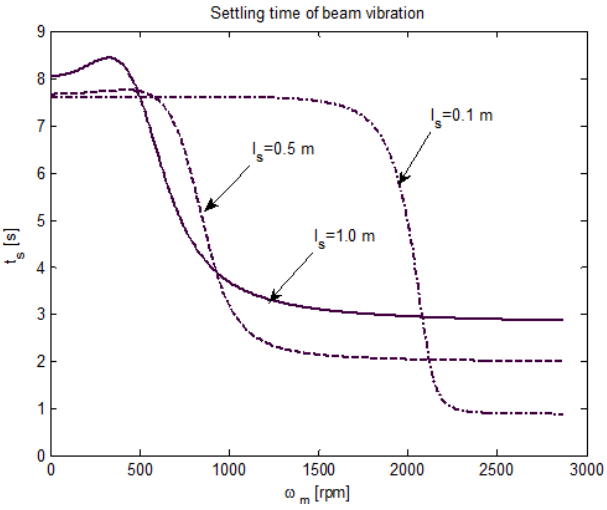

Fig. 4 The settling time of the beam lateral vibration with respect to motor speed

Since the damping ratio ζ_b and the natural frequency ω_b are changing with the motor speed, settling time of the beam lateral vibrations will also change. Settling time plot shows that beam vibration settling time is much shorter when the motor speed reaches the natural frequency of the shaft-disk system ω_T.

Generalized coordinates q_b, q_u and q_s can be written in terms of eigenvalues and eigenvectors as

$$\{q\} = [E][S] \tag{30}$$

Here $\{q\} = \{q_b \quad q_u \quad q_s\}^T$, [$E$] is 3x6 eigenvector matrix and [S] is 6x6 diagonal eigenvalue matrix. For example q_b in open form is

$$q_b = E_{bb}e^{s_b t} + E_{bb}^* e^{s_b^* t} + E_{ub}e^{s_u t} + E_{ub}^* e^{s_u^* t} + E_{sb}e^{s_s t} + E_{sb}^* e^{s_s^* t} \tag{31}$$

Here E_{bb} and E_{bb}^* are complex conjugate eigenvector elements of the beam lateral vibration. s_b and s_b^* are also complex conjugate eigenvalues of the beam lateral vibration which is shown as $s_{1,2}$ in (28). E_{ub} and E_{ub}^* are complex conjugate eigenvector components which are the contribution of the longitudinal beam vibration to the lateral beam vibration. s_u and s_u^* are eigenvectors which are complex conjugate eigenvalues of the beam longitudinal vibration which are $s_{3,4}$ in (28). E_{sb} and E_{sb}^* are complex conjugate eigenvector components which are the contribution of the torsional vibration to the lateral beam vibration. s_s and s_s^* are eigenvectors which are complex conjugate eigenvalues of the flexible shaft torsional vibration which are $s_{5,6}$ in (28).

Similar to (31) equations for $q_u(t)$ and $q_s(t)$ can also be written. Equation (31) can be put in more familiar format by using algebra and trigonometric identities such as

$$\begin{aligned} q_b(t) = {} & X_{bb}e^{-\zeta_b \omega_b t}\sin\left(\omega_b\sqrt{1-\zeta_b^2}\,t + \Phi_{bb}\right) + \\ & X_{ub}e^{-\zeta_u \omega_u t}\sin\left(\omega_u\sqrt{1-\zeta_u^2}\,t + \Phi_{ub}\right) + \\ & X_{sb}e^{-\zeta_s \omega_T t}\sin\left(\omega_T\sqrt{1-\zeta_s^2}\,t + \Phi_{sb}\right) \end{aligned} \tag{32}$$

Here X_{bb} is the modal amplitude contributed by beam lateral vibration, Φ_{bb} is the phase angle, X_{ub} is the modal amplitude contributed by the longitudinal vibration of the beam, Φ_{ub} is the phase angle and X_{sb} is the modal amplitude contributed by the shaft vibration, Φ_{sb} is the phase angle. Similar equations can be written for $q_u(t)$ and $q_s(t)$ such as

$$\begin{aligned} q_u(t) = {} & X_{bu}e^{-\zeta_b \omega_b t}\sin\left(\omega_b\sqrt{1-\zeta_b^2}\,t + \Phi_{bu}\right) + \\ & X_{uu}e^{-\zeta_u \omega_u t}\sin\left(\omega_u\sqrt{1-\zeta_u^2}\,t + \Phi_{uu}\right) + \\ & X_{su}e^{-\zeta_s \omega_T t}\sin\left(\omega_T\sqrt{1-\zeta_s^2}\,t + \Phi_{su}\right) \end{aligned} \tag{33}$$

$$q_s(t) = X_{bs}e^{-\zeta_b\omega_b t}\sin\left(\omega_b\sqrt{1-\zeta_b^2}t+\Phi_{bs}\right)+$$
$$X_{us}e^{-\zeta_u\omega_u t}\sin\left(\omega_u\sqrt{1-\zeta_u^2}t+\Phi_{us}\right)+ \quad (34)$$
$$X_{ss}e^{-\zeta_s\omega_T t}\sin\left(\omega_T\sqrt{1-\zeta_s^2}t+\Phi_{ss}\right)$$

Fig. 5 shows modal amplitudes of the beam lateral vibration X_{bb}, X_{ub} and X_{sb} with respect to the motor speed ω_m. To fit the three modal amplitudes in the same plot, their magnitudes are changed to *dB*. Modal amplitudes and phase angles are calculated for shaft length of 0.1 m. For small values of the motor speed, the contribution of the longitudinal vibration to the lateral vibration of the beam is very high while the contribution of the shaft vibration is small. When the motor speed is increased, the magnitude of X_{ub} is decreased and the magnitude of X_{sb} is increased, but at the same time X_{bb} is also increased.

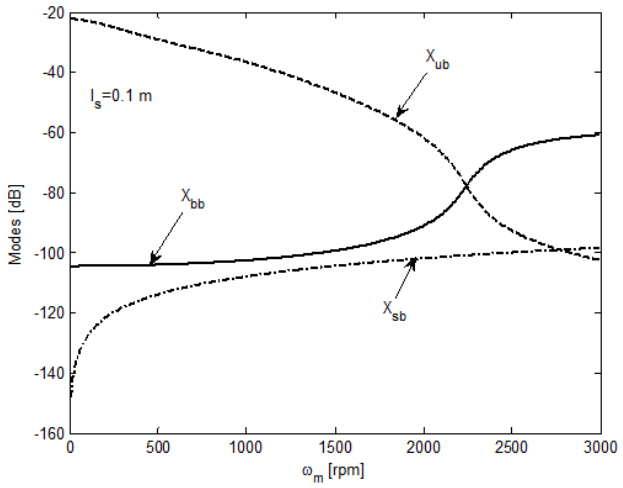

Fig. 5 Modal amplitudes of the beam lateral vibration with respect to motor speed

Fig. 6 shows the change of phase angles Φ_{bb}, Φ_{ub} and Φ_{sb} with respect to the motor speed. Phase angles stay almost constant but small change in the phase angles Φ_{bb} and Φ_{ub} can be seen around the motor speed 2000 to 2500 rpm.

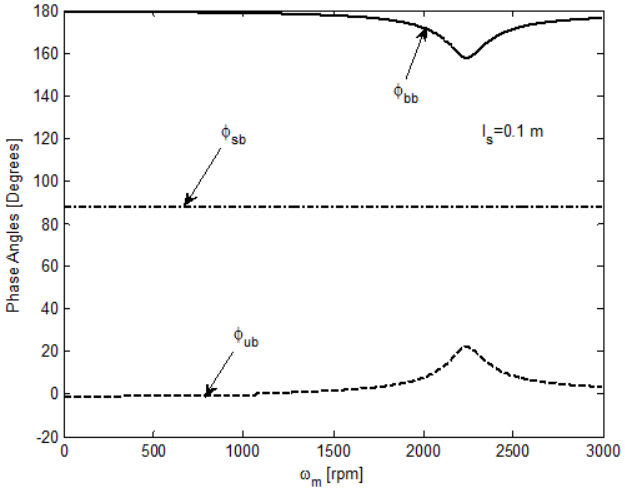

Fig. 6 Phase angles of the beam lateral vibration with respect to motor speed

Fig. 7 shows the modal amplitudes of the beam longitudinal vibration X_{bu}, X_{uu} and X_{su}.The modal amplitude X_{su} is not changing with the motor speed but X_{uu} decreases and X_{bu} increases approximately after motor speed 2000 rpm.

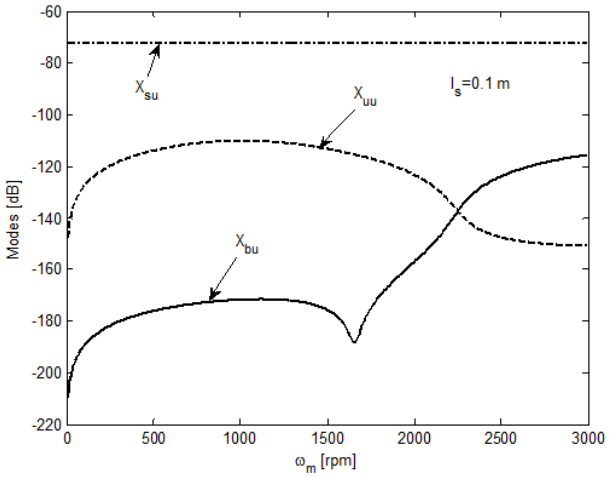

Fig. 7 Modal amplitudes of the beam longitudinal vibration with respect to motor speed

Fig. 8 shows the phase angles Φ_{bu}, Φ_{uu} and Φ_{su} of the beam longitudinal vibration. The phase angle Φ_{su} is not changing by the motor speed but the beam lateral vibration phase angle Φ_{bu} changes approximately from -90° to +90° after motor speed 1500 rpm.

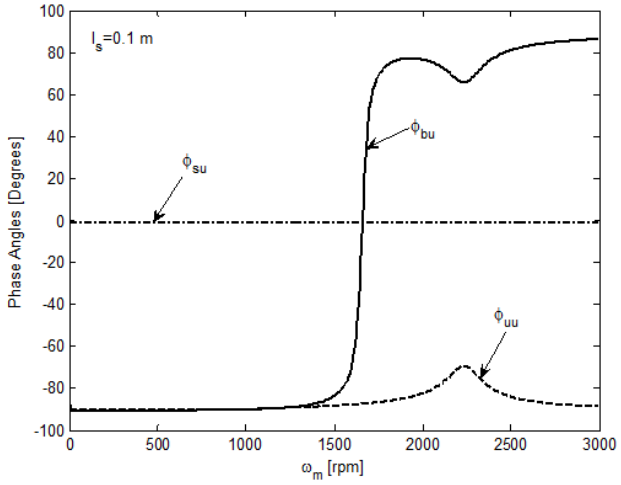

Fig. 8 Phase angles of the beam longitudinal vibration with respect to motor speed

Fig. 9 shows the modal amplitudes of shaft torsional vibration which are X_{bs}, X_{us} and X_{ss}. These modal amplitudes are not changing appreciably by the motor speed.

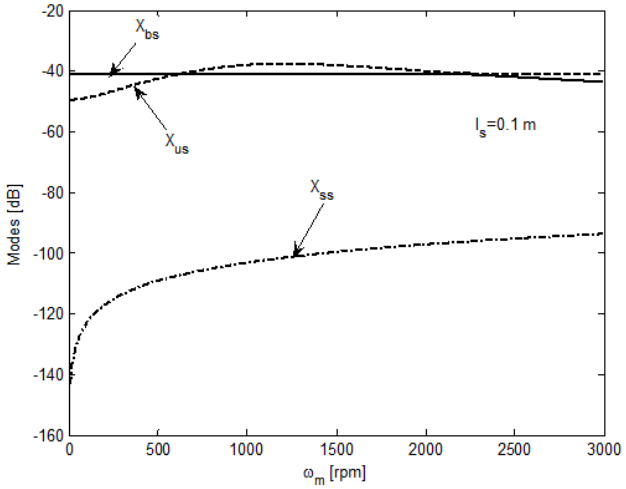

Fig. 9 Modal amplitudes of the shaft vibration with respect to motor speed

Fig. 10 shows the phase angles of the shaft torsional vibration. Similar to the modal amplitudes, the phase angles Φ_{bs}, Φ_{us} and Φ_{ss} are also not changing with the motor speed. Dynamic equation of the longitudinal vibration of beam has a forcing function on the right side, which is shown as f_2 in (26). This force is a centrifugal force that excites the vibrations of the system.

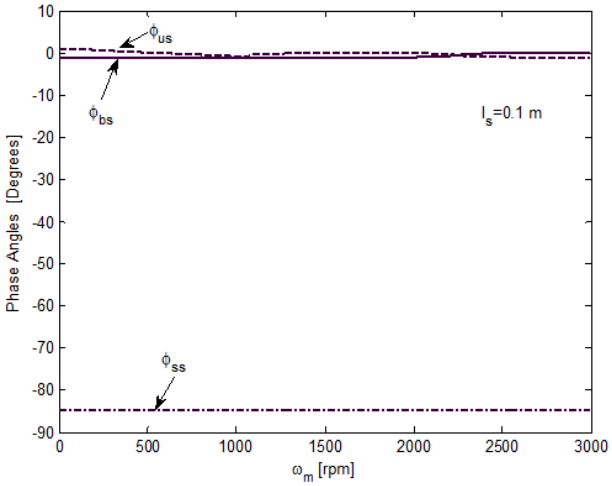

Fig. 10 Phase angles of the shaft vibration with respect to motor speed

As an example Fig. 11, Fig. 12 and Fig. 13 are plotted to show the beam lateral and longitudinal vibrations and torsional vibrations for motor speed of 3000 rpm and shaft length of 0.1 m. Since the beam longitudinal vibration natural frequency is very high settling time of longitudinal vibration is relatively short, it damps out around 0.03 second.

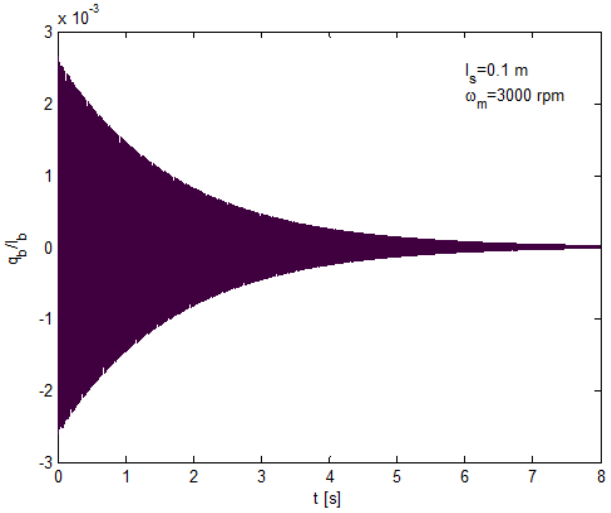

Fig. 11 The beam lateral vibration for motor speed 3000 rpm

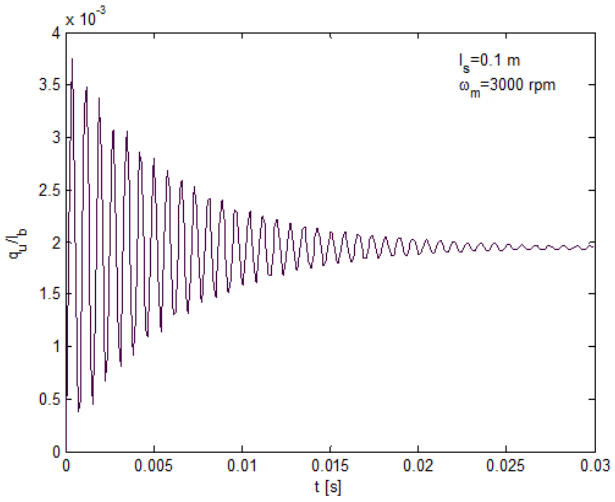

Fig. 12 The beam longitudinal vibration for motor speed 3000 rpm

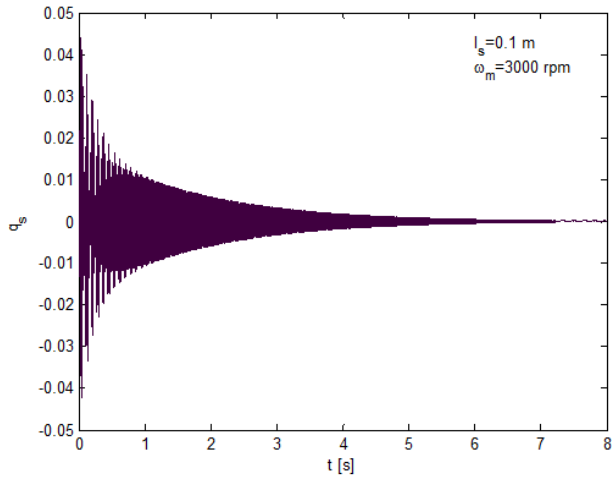

Fig. 13 The shaft torsional vibration for motor speed 3000 rpm

IV. Conclusion

In this work, rotating flexible shaft-disk system having flexible beams is considered as a dynamic system. Equations of the dynamic system are derived considering that the shaft is driven with a motor of speed ω_m. After neglecting nonlinear terms, torsional vibration of the shaft-disk system and lateral and longitudinal vibration of the flexible beam are still coupled through the motor speed. The system has three natural frequencies; the flexible shaft-disk system torsional natural frequency, the flexible beam lateral and longitudinal natural frequencies. Eigenvalue calculations show that while the motor speed changes the shaft-disk system torsional natural frequency and the beam longitudinal natural frequency is not changing but the beam lateral natural frequency changes.

Results show that the beam lateral natural frequency stays the same as the nonrotating beam lateral natural frequency ω_b until the motor speed ω_m is equal to ω_b. After then ω_b increases and remains equal to the motor speed ω_m until the motor speed is equal to the shaft-disk system natural frequency of ω_T. Then the beam lateral natural frequency ω_b becomes equal to the natural frequency ω_T and stays same while the motor speed ω_m is increased. Since the system is coupled, each vibration is the combination of the three vibrations with modal amplitude values and phase angles. These modal amplitudes and phase angles are also plotted against the motor speed.

References

[1] Al Bedoor B. O., Al Sinawi A. and Hamdan M. N. "Nonlinear Dynamic Model of an Inextensible Rotating Flexible Arm Supported on a Flexible Base" *Journal of Sound and Vibration*, 2002, Vol. 251, pp. 767-781.

[2] Al Nassar Y. M., Al Bedoor B. O. and Hamdan M. N. "On the Vibration of a Rotating Blade on a Torsionally Flexible Shaft" *Journal of Sound and Vibration*, 2002, Vol. 259, pp. 1237-1242.

[3] Al Sinawi A. and Hamdan M. N. "Optimal Vibration Estimation of a Nonlinear Flexible Beam Mounted on a Rotating Compliant Hub" *Journal of Sound and Vibration*, 2003, Vol. 259, pp. 857-872.

[4] Alnefaie K. "Effect of Servomotor Control Parameters on the Dynamic Behavior of a Coupled Elastic Shaft Elastic Beam System" *Int. Journal of Vehicle Noise and Vibration*, 2007, Vol. 3, pp. 339-354.

[5] Diken H. and Ankarali A. "Vibration Control of an Elastic Manipulator Link" *Journal of Sound and Vibration*, 1997, Vol. 204, pp. 162-170.

[6] Diken H. "Dynamic Behavior of a Coupled Elastic Shaft Elastic Beam System" *Journal Of Sound and Vibration*, 2006, Vol. 293, pp. 1-15.

[7] Diken H. "Frequency Response Characteristics of a Single link Flexible Joint Manipulator and Possible Trajectory Tracking" *Journal of Sound and Vibration*, 2000, Vol. 233, pp. 179-194.

[8] Diken H. "Precise Trajectory Tracking Control of Elastic Joint Manipulator" *AIAA Journal of Guidance*, 1996, Vol. 19, pp. 715-718.

[9] Diken H. "Servomotor Control of a Coupled Elastic Shaft Elastic Beam System" *Mechanism and Machine Theory*, 2007, Vol. 42, pp. 1376-1387.

[10] Diken H. "Vibration Control of a Rotating Euler Bernoulli Beam" *Journal of Sound and Vibration*, 2000, Vol. 232, pp. 541-551.

[11] Kopmaz O. and Anderson K. S. "On the Eigen-Frequencies of a Flexible Arm Driven by a Flexible Shaft" *Journal of Sound and Vibration*, 2001, Vol. 240, pp. 679-704.

[12] Xi F. and Fenton R. G. "Coupling Effect of Flexible Link and Flexible Joint" *Int. Journal of Robotics Research*, 1994, Vol. 13, pp. 443-453.

[13] Xi F., Fenton R. G. and Tabarrok B. "Coupling Effects in a Manipulator with both a Flexible Link and Joint" *Journal of Dynamic Systems, Measurement, and Control*, 1994, Vol. 116, pp. 826-831.

Dr. Khaled Alnefaie has been born in Taif, Saudi Arabia, 1967. He has obtained his Bachelor degree from the Department of Mechanical Engineering at King Abdulaziz University, Jeddah, Saudi Arabia in 1991. He has obtained his PhD in Mechanical Engineering from the University of Central Florida, Orlando, Florida, USA in 2000. He is currently an associate professor in the Department of mechanical engineering at King Abdulaziz University, Jeddah, Saudi Arabia and He is the Chairman of the Department. His research interests include rotor dynamics, robotics, modal analysis, vibrations, and damage detection.